Box-based Temporal Decomposition of Multi-period Economic Dispatch for Two-stage Robust Unit Commitment

Youngchae Cho, Takayuki Ishizaki, *Member, IEEE,* Nacim Ramdani, *Member, IEEE,*
and Jun-ichi Imura, *Senior Member, IEEE*

Abstract—To ensure the feasibility of a unit commitment (UC) schedule under uncertainty, most existing two-stage robust UC methods formulate their second-stage problems as a multi-period economic dispatch (ED) problem with dynamic constraints, which does not properly model real-time ED where dynamic constraints relevant to the future operation are not certifiable. This paper proposes a two-stage robust UC method where a UC schedule and a box in a feasible operation set of each power source as its new feasible operation set are determined. As the multi-period ED problem with the refined feasible set at the second stage has no dynamic constraint, it is identical to a series of single-period ED problems. By modeling real-time ED as the single-period ED problems whose solutions depend only on uncertainties at the corresponding timeslots, the proposed method presents a practical framework of non-anticipative robust UC. Simulation results with a 118-bus system demonstrate the performance of the proposed method.

Index Terms—Cut generation algorithm, multi-period economic dispatch, non-anticipativity, robust unit commitment.

I. INTRODUCTION

A. Unit Commitment under Uncertainty

UNIT commitment (UC) is a family of mathematical optimization problems to determine the operating states of dispatchable generators (DGs) in a power system, whose objective is to minimize the total operational cost, i.e., start-up/shut-down costs plus dispatch costs of the DGs, over a given planning horizon. As DGs cannot be turned on or off quickly, a UC problem is formulated and solved in advance, e.g., one day or a week ahead of the operating day. Thus, various types of real-time information that cannot be predicted precisely, such as load, renewable generation, and component failure, must be modeled properly in a UC problem to ensure a reasonable degree of power system reliability. With this background, many UC methods have been proposed in the literature to deal with uncertainties, most of which include an economic dispatch (ED) problem for one or more scenarios to consider the total operational cost according to their own criteria.

Y. Cho, T. Ishizaki, and J. Imura are with the Department of Systems and Control Engineering, School of Engineering, Tokyo Institute of Technology, Tokyo, Japan e-mails: {cho,ishizaki,imura}@cyb.sc.e.titech.ac.jp.

N. Ramdani is with Univ. Orléans, INSA-CVL, PRISME EA 4229, F45072, Orléans, France e-mail: nacim.ramdani@univ-orleans.fr

B. Literature Review

A common technique for UC with uncertainty is two-stage stochastic programming. In two-stage stochastic UC, a UC decision is made at the first stage so that the expected ED cost is minimized at the second stage for a given set of scenarios with a known probability distribution. Relevant studies include [1], [2]. In [1], uncertain demand response is represented as scenarios. In [2], the impact of large-scale wind integration is studied with wind power production modeled as scenarios. While many existing algorithms such as Benders decomposition [3] and its variations can be applied with good computational performances [4], [5], identifying the probability distribution of uncertainty is not easy.

Another frequent approach for UC under uncertainty is two-stage robust optimization, where the uncertainty is assumed to be in a given set without considering its probability distribution. In two-stage robust UC, a UC decision is made at the first stage so that the worst-case ED cost is minimized for the uncertainty set at the second stage. The relevant recent studies include [6]–[15]. In [6], the worst-case scenario of wind power fluctuation with deterministic loads is considered. In [7], the UC decision considers all possible amounts of future net injection in a given uncertainty set. In [8], uncertainty of the price elasticity of demand is considered. In [9], both the wind power and the price-elastic demand curve are allowed to vary. In [10], the uncertainties of market price and wind generation are addressed. In [11], the weighted sum model of the two-stage stochastic and robust UC methods is presented. In [12], dispatchable wind power is considered in the weighted sum model. The two-stage robust UC framework is used to handle the component failure uncertainty as well. In [13], a method is proposed to ensure power balance under the concurrent loss of up to a given number of DGs in a single-bus power system. Based on this study, both DG and transmission-line outages in a multi-bus power system are considered in [14] and a probability distribution of a DG failure is introduced in [15]. For comprehensive reviews and comparisons of two-stage stochastic and robust UC frameworks, see [16] and [17].

While considerable advances have been made in the two-stage UC methods, their main drawback remains that they do not model real-time ED at each separate timeslot properly. As the ED problem at the second stage is a multi-period problem with dynamic or intertemporal constraints such as ramp-rate limits of DGs over the planning horizon, the ED solution at

any timeslot in the two-stage UC frameworks is a function of a time series of the uncertainty over the planning horizon. This indicates that the past ED solutions as well as the current ED solution are optimized, which is impractical because the past ED solutions must be given constants for any type of real-time ED.

The same issue arises in many reserve-based UC methods, e.g., [18]–[20], most of which do not explicitly consider the dynamic constraint of power outputs by DGs, i.e., ramping limits, after a reserve is activated. Particularly, while it is possible to change the power output by a DG at a timeslot as a base-case ED solution by using a spinning reserve, it is uncertain if an ED solution exists in the feasible range of power output by the DG at the subsequent timeslot. This is because the dynamic constraint of the power output of the DG over the two adjacent timeslots is enforced only for the base-case ED solution, i.e., in the case where no reserve is used.

UC methods modeling real-time ED at each timeslot to overcome this "non-anticipativity" issue in the conventional UC frameworks include [21]–[25]. In [21], [22], stochastic programming is used with a scenario tree, where each node corresponds to real-time ED at each timeslot for each scenario, ensuring that a real-time ED solution exists for any scenario. However, the curse of dimensionality regarding the number of scenarios is yet to be addressed, i.e., the number of scenarios increases exponentially with that of nodes at each timeslot. In [23], an interval analysis is adopted to allow for any load fluctuation over two adjacent timeslots for a box load uncertainty set. Although not modeling a real-time ED problem explicitly, this method can ensure system reliability for any load scenario and its fluctuation. In [24], a real-time ED solution at each timeslot is modeled as an affine function of the current and past load uncertainties. The coefficients and constant term of each function are optimized together with the UC decision via multi-stage robust optimization. This technique is extended in [25] with temporal and spatial dynamics of uncertain wind and solar generation considered.

C. Contribution

This paper proposes a two-stage robust UC method for a DC power system under load and DG outage uncertainties, which models real-time ED at any timeslot as a non-anticipative single-period problem. In the proposed two-stage method, a UC schedule and a box in a feasible operation set of each DG are determined at the first stage. Each box is identified with the upper and lower limits of power output by a corresponding DG at the timeslots. At the second stage, the boxes form a new feasible set of the multi-period ED problem, combined with a part of the original feasible set, where the operations of the DGs and uncertainties are spatially coupled. Note that a feasible range of any scalar variable is independent of the other scalar variables over each box, which indicates that there is no dynamic constraint. Subsequently, the refined multi-period ED problem can be identically decomposed as a series of single-period ED problems where the operations of the DGs and uncertainties at a single timeslot are coupled

only spatially. Thus, each single-period ED problem can be regarded as a real-time ED problem at each separate timeslot. Consequently, as the feasibility of each single-period ED problem is unaffected by a load realization at another timeslot, the proposed method can ensure that its UC solution is feasible for any load realization over the planning horizon, combined with the refined feasible operation set of each DG. The first-stage decision variables, i.e., the UC schedule and boxes, are determined so that the worst-case total operational cost is minimized over the planning horizon. The load uncertainty set is modeled as a box, which indicates that the loads are spatiotemporally independent in terms of their users' decision-making regarding how much power to consume. Furthermore, the contingency criterion for the system to endure the simultaneous loss of a given number of DGs is applied. Moreover, the power output and input operations by energy storage systems (ESSs) are modeled as well similarly, which are increasingly integrated to accommodate the variability of a large penetration of renewable generation efficiently [26].

The proposed method has advantages over the aforementioned UC methods [1], [2], [4]–[15], [18]–[25] in several ways; it explicitly addresses the non-anticipativity issue in [1], [2], [4]–[15], [18]–[20]; it does not suffer from the curse of dimensionality in [21], [22], as it is a robust-optimization-based approach and does not specify each scenario; it can model an ESS, which is not easy in [23] as the dynamic constraint for the storage capacity of an ESS is effective over all the timeslots as a whole, not over two adjacent timeslots as in the case of the ramp-rate limits of DGs; it can incorporate a contingency criterion for the DG outage, which is not straightforward in [24], [25] where the ED policy of each DG is based on a predetermined affine function of net-load uncertainties.

D. Layout

The remainder of this paper is structured as follows. In Section II, a deterministic UC problem and a conventional two-stage robust UC problem are described first, and subsequently, the novel two-stage robust UC problem is formulated. In Section III, a cut-generation algorithm for solving the problem is presented. Numerical experiment results are discussed in Section IV. Section V concludes the paper.

II. PROBLEM FORMULATION

This section presents a novel two-stage robust UC problem where real-time ED under load and DG outage uncertainties is modeled. Before the problem statement, a deterministic UC problem and a conventional two-stage robust UC problem only for the load uncertainty are described in the following two subsections for better understanding of the validity of the proposed method.

As for the DC power system considered, the bus and transmission line index sets are denoted by $\mathcal{I} := \{1, \ldots, N\}$ and $\mathcal{L}$, respectively. Without loss of generality, it is assumed that a DG, ESS, and load, all with the index i, are connected to bus i for all $i \in \mathcal{I}$. While not modeled explicitly, a non-dispatchable renewable generator can be considered as a load

with a negative load value. The planning horizon contains T timeslots with unit length, whose index set is denoted by $\mathcal{T}$. Any real number with a double subscript it indicates that it is concerned with bus i and timeslot t.

A. Deterministic UC

A UC decision to minimize the total operational cost for given loads d_{it} for all $i \in \mathcal{I}$ and $t \in \mathcal{T}$ can be made as a solution of the mixed-integer linear programming (MILP) problem

$$\min_{u_{it}, v_{it}, w_{it}, x_{it}, y_{it}^{\mathrm{i}}, y_{it}^{\mathrm{o}}} \sum_{t \in \mathcal{T}} \sum_{i \in \mathcal{I}} \left(C_i^{\mathrm{n}} u_{it} + C_i^{\mathrm{su}} v_{it} + C_i^{\mathrm{sd}} w_{it} \right.$$
$$\left. + C_i^{\mathrm{g}} x_{it} + C_i^{\mathrm{i}} y_{it}^{\mathrm{i}} + C_i^{\mathrm{o}} y_{it}^{\mathrm{o}} \right) \tag{1a}$$

$$\text{s.t.} \quad v_{it} \geq u_{it} - u_{i(t-1)}, \quad \forall i \in \mathcal{I}, \forall t \in \mathcal{T}, \tag{1b}$$

$$w_{it} \geq -u_{it} + u_{i(t-1)}, \quad \forall i \in \mathcal{I}, \forall t \in \mathcal{T}, \tag{1c}$$

$$u_{it} - u_{i(t-1)} \leq u_{i\tau},$$
$$t \leq \tau \leq \min\left\{t - 1 + T_i^{\mathrm{u}}, T\right\}, \quad \forall i \in \mathcal{I}, \forall t \in \mathcal{T}, \tag{1d}$$

$$u_{i(t-1)} - u_{it} \leq 1 - u_{i\tau},$$
$$t \leq \tau \leq \min\left\{t - 1 + T_i^{\mathrm{d}}, T\right\}, \quad \forall i \in \mathcal{I}, \forall t \in \mathcal{T}, \tag{1e}$$

$$u_{it}, v_{it}, w_{it} \in \{0, 1\}, \quad \forall i \in \mathcal{I}, \forall t \in \mathcal{T} \tag{1f}$$

$$X_i^{\min} u_{it} \leq x_{it} \leq X_i^{\max} u_{it}, \quad \forall i \in \mathcal{I}, \forall t \in \mathcal{T}, \tag{1g}$$

$$-X_i^{\mathrm{d}} u_{it} - X_i^{\mathrm{sd}} w_{it} \leq x_{it} - x_{i(t-1)}$$
$$\leq X_i^{\mathrm{u}} u_{i(t-1)} + X_i^{\mathrm{su}} v_{it}, \quad \forall i \in \mathcal{I}, \forall t \in \mathcal{T}, \tag{1h}$$

$$0 \leq y_{it}^{\mathrm{i}} \leq Y_i^{\mathrm{i}}, \quad \forall i \in \mathcal{I}, \forall t \in \mathcal{T}, \tag{1i}$$

$$0 \leq y_{it}^{\mathrm{o}} \leq Y_i^{\mathrm{o}}, \quad \forall i \in \mathcal{I}, \forall t \in \mathcal{T}, \tag{1j}$$

$$0 \leq S_{i0} + \sum_{\tau=1}^{t} \left(E_i^{\mathrm{i}} y_{it}^{\mathrm{i}} - \frac{1}{E_i^{\mathrm{o}}} y_{it}^{\mathrm{o}} \right) \leq S_i,$$
$$\forall i \in \mathcal{I}, \forall t \in \mathcal{T}, \tag{1k}$$

$$F_l^{\min} \leq \sum_{i \in \mathcal{I}} F_{li} \left(x_{it} - y_{it}^{\mathrm{i}} + y_{it}^{\mathrm{o}} - d_{it} \right) \leq F_l^{\max},$$
$$\forall l \in \mathcal{L}, \forall t \in \mathcal{T}, \tag{1l}$$

$$\sum_{i \in \mathcal{I}} \left(x_{it} - y_{it}^{\mathrm{i}} + y_{it}^{\mathrm{o}} - d_{it} \right) = 0, \quad \forall t \in \mathcal{T} \tag{1m}$$

where the binary variables u_{it}, v_{it}, and w_{it} are the indicators of on/off, start-up, and shut-down states, respectively, of DG i at timeslot t; x_{it} is the power output by DG i at timeslot t; y_{it}^{i} and y_{it}^{o} are the power input to and output by ESS i at timeslot t, respectively.

In the objective function (1a), C_i^{n}, C_i^{su}, C_i^{sd}, and C_i^{g} represent the no-load, start-up, shut-down, and marginal generation costs of DG i, respectively; C_i^{i} and C_i^{o} represent the power input and output costs of ESS i, respectively. The constraints (1b) and (1c) represent the start-up and shut-down operations, respectively, of the DGs; (1d) and (1e) describe the minimum up and down time constraints of the DGs, respectively, with T_i^{u} and T_i^{d} denoting the minimum up and down times of DG i, respectively; (1g) represents the generation capacities of the DGs with $X_i^{\min}$ and $X_i^{\max}$ denoting the minimum and maximum power outputs of DG i, respectively; (1h) represents the ramp-up and ramp-down constraints of DGs

with X_i^{u}, X_i^{su}, X_i^{d}, and X_i^{sd} denoting the ramp-up, start-up-ramp, ramp-down, and shut-down-ramp limits of DG i, respectively; (1i) and (1j) represent the feasible power input and output ranges of the ESS, respectively, with Y_i^{i} and Y_i^{o} denoting the maximum power input to and output by ESS i, respectively; (1k) represents the storage capacity constraints of the ESSs with S_{i0}, E_i^{i}, E_i^{o}, and S_i denoting the initial stored energy, input and output efficiencies, and storage capacity of ESS i, respectively; (1l) represents the transmission line capacities with $F_l^{\min}$, $F_l^{\max}$, and F_{li} denoting the minimum and maximum real power flows in transmission line l and DC power transfer distribution factor between bus i and transmission line l, respectively; (1m) represents the power supply–demand balance equations.

The problem (1) can be rewritten in a compact form as

$$\min_{\boldsymbol{u} \in \mathcal{U}, x \in \mathcal{X}(\boldsymbol{u}), y \in \mathcal{Y}} C_1^{\mathrm{T}} \boldsymbol{u} + C_2^{\mathrm{T}} x + C_3^{\mathrm{T}} y$$
$$\text{s.t.} \quad (x, y) \in \mathcal{S}(d) \tag{2}$$

where $\boldsymbol{u}$ is a vector of the binary variables u_{it}, v_{it}, and w_{it} for all $i \in \mathcal{I}$ and $t \in \mathcal{T}$; x is a vector of the real variables x_{it}; y is a vector of the real variables y_{it}^{i} and y_{it}^{o}; the vectors C_1, C_2, and C_3 include the cost coefficients in (1a) of the corresponding variables, representing the total UC cost, total ED cost incurred by the DGs, total ED cost incurred by the ESSs, and total penalty, respectively. The set $\mathcal{U} := \{\boldsymbol{u} : \text{(1b)-(1f)}\}$ includes all feasible UC schedules of the DGs; $\mathcal{X}(\boldsymbol{u}) := \{x : \text{(1g),(1h)}\}$ is a set of feasible operations of the DGs for $\boldsymbol{u}$; $\mathcal{Y} := \{y : \text{(1i), (1j), (1k)}\}$ is a set of feasible operations of the ESSs; d is a vector of d_{it} and $\mathcal{S}(d) := \{(x, y) : \text{(1l), (1m)}\}$ is a set of feasible ED schedules in terms of the spatial constraints in the entire system for d.

The solution of (1) does not ensure the system reliability under load uncertainty because it considers only a single load scenario d. The conventional two-stage robust UC method for load uncertainty is described in the following subsection, based on which the proposed method is formulated.

B. Conventional Two-stage Robust UC

Suppose that the vector d is uncertain while belonging to a box $\mathcal{D} := \left\{d : \underline{d} \leq d \leq \overline{d}\right\}$ where $\underline{d}$ and $\overline{d}$ are vectors of the minimum and maximum load values, respectively. Subsequently, a two-stage robust UC problem to minimize the worst-case total operational cost for the load uncertainty set $\mathcal{D}$ is formulated in a conventional way [7] as

$$\min_{\boldsymbol{u} \in \mathcal{U}} \left\{ C_1^{\mathrm{T}} \boldsymbol{u} + \max_{d \in \mathcal{D}} \mathcal{E}_1(\boldsymbol{u}, d) \right\} \tag{3}$$

where $\mathcal{E}_1(\boldsymbol{u}, d)$ is the optimal value of the ED problem

$$\min_{x \in \mathcal{X}(\boldsymbol{u}), y \in \mathcal{Y}} C_2^{\mathrm{T}} x + C_3^{\mathrm{T}} y \quad \text{s.t.} \quad (x, y) \in \mathcal{S}(d). \tag{4}$$

The two-stage structure of the problem (3) indicates that $\boldsymbol{u}$ is determined at the first stage before d is known, and an ED schedule (x, y) is determined via the problem (4) at the second stage after d is given. Note that only $\boldsymbol{u}$ is returned as a solution of (3). Meanwhile, (4) does not model real-time ED in a proper manner, which is a multi-period

problem with the dynamic constraints (1h) and (1k) in $\mathcal{X}(\boldsymbol{u})$ and $\mathcal{Y}$, respectively. Consequently, the actual total operational cost might be higher than the optimal value of (3), or there might not be a feasible ED solution at some timeslot, which undermines the validity of the conventional two-stage robust UC method. To address this issue, the proposed method determines additional variables at the first stage and refines the feasible set of the multi-period ED problem at the second stage so that it can be regarded as a series of real-time ED problems that are always feasible regarding the uncertainty. The details are described in the following subsection.

C. Box-based Decomposition of Multi-period ED

A multi-period ED problem without any dynamic constraint is identical to a series of single-period ED problems. Accordingly, an ED solution at each timeslot is a function of the system parameters, including any uncertainty, at the corresponding timeslot. Thus, each single-period ED problem is a reasonable mathematical model for real-time ED. However, dynamic constraints are intrinsic to both DGs and ESSs. The proposed method replaces the original feasible operation set of each power source by an inner box, which is identified with refined lower and upper limits of its operation at each timeslot. As any pair of operations at different timeslots is independent in the box, the multi-period ED problem can be considered as a series of real-time ED problems over the new feasible set, i.e., the boxes combined with the spatial constraints at each timeslot. A box in the feasible operation set of each power source can be modeled based on the following proposition.

Proposition 1. *Consider a set*

$$\mathcal{C}_1 := \{c \in \mathbb{R}^n : f_p(c) \leq 0, \forall p \in \mathcal{P}\}$$

where $\mathbb{R}$ denotes the real number set, $\mathcal{P}$ is an index set, and $f_p : \mathbb{R}^n \to \mathbb{R}$ for any $p \in \mathcal{P}$ is a convex function. Then, a necessary and sufficient condition for a bounded convex polytope $\mathcal{C}_2$ to belong to $\mathcal{C}_1$ is

$$f_p(c) \leq 0, \ \forall p \in \mathcal{P}, \forall c \in \mathcal{V}(\mathcal{C}_2)$$

where $\mathcal{V}(\mathcal{C}_2)$ is the set of vertices of $\mathcal{C}_2$.

Proof. Noting that any point in a bounded convex polytope can be represented as a convex combination of its vertices, consider a point $c_0 = \sum_{q=1}^{|\mathcal{V}(\mathcal{C}_2)|} \alpha_q c_q$ in $\mathcal{C}_2$ where $\sum_{q=1}^{|\mathcal{V}(\mathcal{C}_2)|} \alpha_q = 1$, $\alpha_q \geq 0$ for any q, and c_q denotes the qth vertex of $\mathcal{C}_2$. Then, it holds that

$$f_p(c_0) \leq \sum_{q=1}^{|\mathcal{V}(\mathcal{C}_2)|} \alpha_q f_p(c_q) \leq 0, \quad \forall p \in \mathcal{P},$$

which indicates that $c_0 \in \mathcal{C}_1$. Since c_0 is arbitrary, the statement holds. ∎

Let $\underline{x}_{it}$ and $\overline{x}_{it}$ denote the new lower and upper limits, respectively, of x_{it} to be determined. According to Proposition

1, a set $[\mathcal{X}](\boldsymbol{u})$ of boxes inside $\mathcal{X}(\boldsymbol{u})$ for a given UC decision $\boldsymbol{u}$ can be represented as

$$[\mathcal{X}](\boldsymbol{u}) := \big\{ [x] := [\underline{x}, \overline{x}] \in \mathbb{IR}^{NT} :$$

$$X_i^{\min} u_{it} \leq \underline{x}_{it} \leq \overline{x}_{it} \leq X_i^{\max} u_{it}, \quad \forall i \in \mathcal{I}, \forall t \in \mathcal{T}, \quad (5\text{a})$$

$$\overline{x}_{it} - \underline{x}_{i(t-1)} \leq X_i^{\mathrm{u}} u_{i(t-1)} + X_i^{\mathrm{su}} v_{it},$$
$$\forall i \in \mathcal{I}, \forall t \in \mathcal{T}, \quad (5\text{b})$$

$$\overline{x}_{i(t-1)} - \underline{x}_{it} \leq X_i^{\mathrm{d}} u_{it} + X_i^{\mathrm{sd}} w_{it}, \ \forall i \in \mathcal{I}, \forall t \in \mathcal{T} \big\}. \quad (5\text{c})$$

where $\underline{x}$ and $\overline{x}$ are vectors of $\underline{x}_{it}$ and $\overline{x}_{it}$, respectively; $\mathbb{IR}$ denotes the set of interval numbers. Similarly, a set $[\mathcal{Y}]$ of boxes in $\mathcal{Y}$ can be represented as

$$[\mathcal{Y}] := \big\{ [y] := [\underline{y}, \overline{y}] \in \mathbb{IR}^{2NT} :$$

$$0 \leq \underline{y}_{it}^{\mathrm{i}} \leq \overline{y}_{it}^{\mathrm{i}} \leq Y_i^{\mathrm{i}}, \quad \forall i \in \mathcal{I}, \forall t \in \mathcal{T}, \quad (6\text{a})$$

$$0 \leq \underline{y}_{it}^{\mathrm{o}} \leq \overline{y}_{it}^{\mathrm{o}} \leq Y_i^{\mathrm{o}}, \quad \forall i \in \mathcal{I}, \forall t \in \mathcal{T}, \quad (6\text{b})$$

$$0 \leq S_{i0} + \sum_{\tau=1}^{t} \left(E_i^{\mathrm{i}} \underline{y}_{i\tau}^{\mathrm{i}} - \frac{1}{E_i^{\mathrm{o}}} \overline{y}_{i\tau}^{\mathrm{o}} \right), \forall i \in \mathcal{I}, \forall t \in \mathcal{T}, \quad (6\text{c})$$

$$S_{i0} + \sum_{\tau=1}^{t} \left(E_i^{\mathrm{i}} \overline{y}_{i\tau}^{\mathrm{i}} - \frac{1}{E_i^{\mathrm{o}}} \underline{y}_{i\tau}^{\mathrm{o}} \right) \leq S_i, \forall i \in \mathcal{I}, \forall t \in \mathcal{T} \big\} \quad (6\text{d})$$

where $\underline{y}$ is a vector of new lower limits $\underline{y}_{it}^{\mathrm{i}}$ and $\underline{y}_{it}^{\mathrm{o}}$ of y_{it}^{i} and y_{it}^{o}, respectively; $\overline{y}$ is a vector of new upper limits $\overline{y}_{it}^{\mathrm{i}}$ and $\overline{y}_{it}^{\mathrm{o}}$ of y_{it}^{i} and y_{it}^{o}, respectively.

Suppose any $\boldsymbol{u} \in \mathcal{U}$, $[x] \in [\mathcal{X}](\boldsymbol{u})$, and $[y] \in [\mathcal{Y}]$ are given. Subsequently, a multi-period ED problem over the boxes for any $d \in \mathcal{D}$ is written as

$$\min_{x \in [x], y \in [y]} C_2^{\mathrm{T}} x + C_3^{\mathrm{T}} y \quad \text{s.t.} \ (x, y) \in \mathcal{S}(d), \quad (7)$$

which is free of dynamic constraints. Thus, if d is uncertain in $\mathcal{D}$, the optimal value of any variable with the timeslot index t is a function of d_{it} for all $i \in \mathcal{I}$. This indicates that the ED solution with the timeslot index t of the problem (7) for any $d \in \mathcal{D}$ is guaranteed to be implementable at timeslot t, which is not the case with (4) where the ED decisions over the planning horizon are co-optimized. Based on the temporal decomposability of (7), a novel two-stage robust UC problem that further incorporates the contingency criterion is formulated in the following subsection.

D. Problem Statement

The objective of this study is to find such boxes $[x]$ and $[y]$ as new feasible operation sets of the power sources that minimize the worst-case total operational cost for the load uncertainty set $\mathcal{D}$ with the contingency criterion allowing for up to κ DGs out of order. Note that the boxes $[x]$ and $[y]$ are identified with the refined maximum and minimum values of the operations of the power sources, i.e., $\overline{x}, \overline{y}, \underline{x}$, and $\underline{y}$. Thus, the boxes can be obtained by solving the problem

$$\min_{\boldsymbol{u} \in \mathcal{U}, \hat{x} \in \hat{\mathcal{X}}(\boldsymbol{u}), \hat{y} \in \hat{\mathcal{Y}}} \left\{ C_1^{\mathrm{T}} \boldsymbol{u} + \max_{d \in \mathcal{D}, h \in \mathcal{H}} \mathcal{E}_2(\hat{x}, \hat{y}, d, h) \right\} \quad (8)$$

where

$$\hat{\mathcal{X}}(\boldsymbol{u}) := \left\{ \hat{x} := \begin{pmatrix} \underline{x} \\ \overline{x} \end{pmatrix} \in \mathbb{R}^{2NT} : \exists [\underline{x}, \overline{x}] \in [\mathcal{X}](\boldsymbol{u}) \right\},$$

$$\hat{\mathcal{Y}} := \left\{ \hat{y} := \begin{pmatrix} \underline{y} \\ \overline{y} \end{pmatrix} \in \mathbb{R}^{2NT} : \exists [\underline{y}, \overline{y}] \in [\mathcal{Y}] \right\},$$

and

$$\mathcal{H} := \left\{ h \in \{0,1\}^N : \sum_{i \in \mathcal{I}} h_i \geq N - \kappa \right\}$$

with h denoting a vector of the binary variables h_i for all $i \in \mathcal{I}$ each of which equals zero, if DG i unexpectedly shuts down, and one, otherwise. The objective function $\mathcal{E}_2(\hat{x}, \hat{y}, d, h)$ of the inner maximization problem is the optimal value of the problem

$$\min_{x \in [x]^c(\hat{x},h), y \in [y]} C_2^T x + C_3^T y \quad \text{s.t.} \quad (x,y) \in \mathcal{S}(d) \qquad (9)$$

where

$$[x]^c(\hat{x}, h) := \{x : \underline{x}_{it} h_i \leq x_{it} \leq \overline{x}_{it} h_i, \forall i \in \mathcal{I}, \forall t \in \mathcal{T}\}$$

denotes the feasible operation set of the DGs for $\hat{x}$ and h. In this study, the problem (9) is assumed to be feasible for any $\boldsymbol{u} \in \mathcal{U}$, $\hat{x} \in \hat{\mathcal{X}}(\boldsymbol{u})$, $\hat{y} \in \hat{\mathcal{Y}}$, $d \in \mathcal{D}$, and $h \in \mathcal{H}$, which can be enforced by introducing penalty terms for any violation of the constraints. An algorithm for solving the problem (8) is described in the following section.

Notably, the load uncertainty set can be modeled as a general convex polytope representing a spatiotemporal correlation of the loads. In this case, however, only a local optimum is guaranteed by the proposed method. To avoid this optimality issue, which remains in the conventional two-stage robust UC method [7] as well, the load uncertainty set is modeled as a box. Further details are explained in the following section and APPENDIX.

III. SOLUTION METHOD

The problem (8) can be solved via Benders decomposition [3], where the original problem is decomposed into two problems that are iteratively solved. In Benders decomposition, the second-stage linear programming (LP) problem (9) is rephrased in its Lagrangian dual form. First, let (9) be rewritten as

$$\min_{\boldsymbol{x} \geq 0} C^T \boldsymbol{x} \quad \text{s.t.} \quad A\boldsymbol{x} \leq a(\hat{x}, h), \qquad (10a)$$

$$B\boldsymbol{x} \leq b(\hat{y}), \qquad (10b)$$

$$D\boldsymbol{x} \leq Ed + e \qquad (10c)$$

where $\boldsymbol{x}$ is a vector concatenating x and y; C is a vector concatenating C_2 and C_3. The constraints (10a) correspond to $x \in [x]^c(\hat{x}, h)$; (10b) represents $y \in \hat{y}$; (10b) represents $(x, y) \in \mathcal{S}(d)$. Thus, the dual form of (9) is written as

$$\max_{\xi \in \Xi} C_4^T(\hat{x}, \hat{y}, d, h) \xi$$

where

$$C_4(\hat{x}, \hat{y}, d, h) := - \begin{pmatrix} a(\hat{x}, h) \\ b(\hat{y}) \\ Ed + e \end{pmatrix}$$

and

$$\Xi := \left\{ \begin{pmatrix} \xi^1 \\ \xi^2 \\ \xi^3 \end{pmatrix} \geq 0 : \begin{pmatrix} A \\ B \\ D \end{pmatrix}^T \begin{pmatrix} \xi^1 \\ \xi^2 \\ \xi^3 \end{pmatrix} + C \geq 0 \right\}$$

with ξ^1, ξ^2, and ξ^3 denoting vectors of the dual variables associated with (10a), (10b), and (10c), respectively. Thus, (8) is rewritten as

$$\min_{\substack{\boldsymbol{u} \in \mathcal{U}, \hat{x} \in \hat{\mathcal{X}}(\boldsymbol{u}), \\ \hat{y} \in \hat{\mathcal{Y}}}} \left\{ C_1^T \boldsymbol{u} + \max_{d \in \mathcal{D}, h \in \mathcal{H}, \xi \in \Xi} C_4^T(\hat{x}, \hat{y}, d, h) \xi \right\}. \quad (11)$$

The inner maximization problem

$$\max_{d \in \mathcal{D}, h \in \mathcal{H}, \xi \in \Xi} C_4^T(\hat{x}, \hat{y}, d, h) \xi \qquad (12)$$

is a mixed-integer non-linear optimization problem for any $\hat{x}$ and $\hat{y}$. Nevertheless, for any fixed h, the problem (12) is an LP problem with regard to $d \in \mathcal{D}$ for any fixed $\xi \in \Xi$ and vice versa. Thus, at least one pair of vertices of $\mathcal{D}$ and Ξ forms a solution of (12) combined with some h and (12) is rewritten as

$$\max_{s \in \{0,1\}^{NT}, h \in \mathcal{H}, \xi \in \Xi} C_4^T\left(\hat{x}, \hat{y}, \underline{d} + s \circ \hat{d}, h\right) \xi$$

where $\hat{d} := \overline{d} - \underline{d}$ and $\circ$ denotes the element-wise product of two vectors; each entry in the binary vector s being equal to one and zero indicates that the corresponding entry in d is equal to its maximum and minimum values, respectively. Subsequently, with an additional variable η, the problem (11) can be represented in a standard form of a minimization problem with a finite number of constraints as

$$\min_{\boldsymbol{u} \in \mathcal{U}, \hat{x} \in \hat{\mathcal{X}}(\boldsymbol{u}), \hat{y} \in \hat{\mathcal{Y}}, \eta} C_1^T \boldsymbol{u} + \eta \qquad (13a)$$

$$\text{s.t.} \quad \eta \geq C_4^T\left(\hat{x}, \hat{y}, \underline{d} + s \circ \hat{d}, h\right) \xi,$$
$$\forall s \in \{0,1\}^{NT}, \forall h \in \mathcal{H}, \forall \xi \in \mathcal{V}(\Xi) \qquad (13b)$$

where $\mathcal{V}(\Xi)$ represents the extreme point set of Ξ. While finite, the number of constraints (13b) is possibly large. Benders decomposition for solving the large-scale problem (13) is described as follows.

For initialization, select some $\boldsymbol{u}_0 \in \mathcal{U}$, $\hat{x}_0 \in \hat{\mathcal{X}}(\boldsymbol{u}_0)$, and $\hat{y}_0 \in \hat{\mathcal{Y}}$ as initial guesses for $\boldsymbol{u}$, $\hat{x}$, and $\hat{y}$, respectively. Subsequently, solve the problem

$$\max_{s \in \{0,1\}^{NT}, h \in \mathcal{H}, \xi \in \Xi} C_4^T\left(\hat{x}_0, \hat{y}_0, \underline{d} + s \circ \hat{d}, h\right) \xi$$

to obtain the maximizers s_0, h_0, and ξ_0. For each iteration step $K \geq 1$, solve the master problem

$$\min_{\boldsymbol{u} \in \mathcal{U}, \hat{x} \in \hat{\mathcal{X}}(\boldsymbol{u}), \hat{y} \in \hat{\mathcal{Y}}, \eta} C_1^T \boldsymbol{u} + \eta \qquad (14a)$$

$$\text{s.t.} \quad \eta \geq C_4^T(\hat{x}, \hat{y}, d_k, h_k) \xi_k, \quad k = 0, 1, \ldots, K-1, \quad (14b)$$

where $d_k := \underline{d} + s_k \circ \hat{d}$, to obtain the solutions $\boldsymbol{u}_K$, $\hat{x}_K$, and $\hat{y}_K$ corresponding to $\boldsymbol{u}$, $\hat{x}$, and $\hat{y}$, respectively. Let LB_K denote the optimal value, which is a lower bound of (13). Subsequently, solve the subproblem

$$\max_{s \in \{0,1\}^{NT}, h \in \mathcal{H}, \xi \in \Xi} C_4^T\left(\hat{x}_K, \hat{y}_K, \underline{d} + s \circ \hat{d}, h\right) \xi \qquad (15)$$

to obtain the solutions s_K, h_K, and ξ_K. Let

$$UB_K := C_1^T \boldsymbol{u} + C_4^T(\hat{x}_K, \hat{y}_K, d_K, h_K)$$

denote the optimal value, which is an upper bound of (13). If

$$UB_K - LB_K < \varepsilon,$$

where $\varepsilon > 0$ is a convergence tolerance, the iteration stops and $\boldsymbol{u}_K$, $\hat{x}_K$, and $\hat{y}_K$ are returned as a solution of (8); otherwise, K increases to $K + 1$ and the problems (14) and (15) are solved again. Note that this method yields the solution in a finite number of iterations because (13) has a finite number of constraints.

Meanwhile, solving (15), which is a mixed-integer programming problem with the bilinear terms of h and ξ^1, and of s and ξ^3, is not straightforward. In this study, each bilinear term is equivalently converted to a real variable with additional constraints [27]. Specifically, a bilinear term $h_i\xi'$ where ξ' is an entry of ξ^1 is equivalently converted to a real variable ζ' constrained by

$$0 \le \zeta' \le Gh_i,$$
$$\xi' - (1 - h_i)G \le \zeta' \le \xi'$$

where G is a large number. Let ζ^1 and $Z(h, \xi^1)$ denote a vector of such additional variables for the bilinear terms regarding h and ξ^1 and its feasible set, respectively. Furthermore, let ζ^3 and $Z(s, \xi^3)$ denote a vector of additional variables for the bilinear terms regarding s and ξ^3 and its feasible set, respectively, which can be described similarly. Thus, (15) is rewritten as the MILP problem

$$\max_{\substack{s\in\{0,1\}^{NT}, h\in\mathcal{H}, \xi\in\Xi, \\ \zeta^1\in Z(h,\xi^1), \zeta^3\in Z(s,\xi^3)}} C_5\left(\hat{x}_K, \hat{y}_K, \zeta^1, \zeta^3, \xi^2, \xi^3\right) \quad (16)$$

where
$$C_5\left(\hat{x}_K, \hat{y}_K, \zeta^1, \zeta^3, \xi^2, \xi^3\right) :=$$
$$- a^{\mathrm{T}}(\hat{x}_K, \mathbf{1})\zeta - b^{\mathrm{T}}(\hat{y}_K)\xi^2 - (E\underline{d} + e)^{\mathrm{T}}\xi^3 - \left(E\hat{d}\right)^{\mathrm{T}}\zeta^3$$

with $\mathbf{1}$ denoting the N-dimensional vector of ones. Fig. 1 describes Benders decomposition for solving (8).

Note that (12) can be solved via the outer approximation algorithm [28] at the expense of global optimality when $\mathcal{D}$ is a general convex polytope; see APPENDIX for details. Note also that the column-constraint generation algorithm [29] can be used to solve (8) as well, where a cut associated with primal variables regarding each pair of d_K and h_K is added to the master problem instead of the one with the dual optimal solutions as in (14b). Numerical experiments were conducted to test the proposed method, where both dual and primal cuts were added to the master problem as it showed faster convergences than when either of them was used separately. The simulation results are discussed in the following section.

IV. NUMERICAL EXPERIMENTS

In this section, the performance of the proposed method is demonstrated via numerical experiments. In the first subsection, boxes as new feasible operation sets of the power sources in a 5-bus system obtained using the proposed method are illustrated to show that the proposed method is appropriate in terms of its non-anticipativity under the uncertainties compared with the conventional two-stage robust UC and reserve-based methods. In the second and third subsections, the
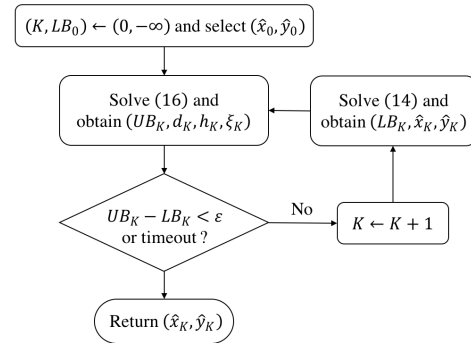
Fig. 1. Benders decomposition for solving the problem (8).
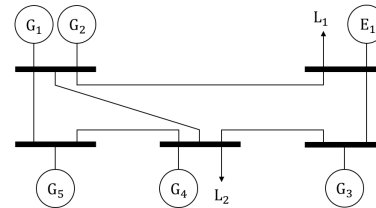
Fig. 2. Modified MATPOWER 5-bus test case.

computational performance and conservatism of the proposed method are discussed in comparison with those of the conventional two-stage robust UC and deterministic UC methods, respectively, with a 118-bus system. All the experiments were run on a computer with an Intel Core i7 processor at 2.6 GHz using 8 GB of RAM, using MATLAB R2016b with CPLEX 12.6.

A. Illustrative Example

This subsection illustrates the non-anticipativity of the proposed method for the 5-bus system in Fig. 2, which is a modified version of the MATPOWER 5-bus test case [30]. The system has five DGs denoted by G_1, G_2, G_3, G_4, and G_5, whose operational parameters are listed in TABLE I with the indices omitted. The DGs are initially turned off. The system also has an ESS denoted by E_1, whose operational parameters are listed in TABLE II. There are two loads denoted by L_1 and L_2 as well. The uncertainty sets of the loads over a planning horizon of six timeslots are shown in Fig. 3. As for the contingency criterion, the system should be reliable not only in a normal state but under the outage of up to two DGs, i.e., $\kappa = 2$.

For this system, the conventional two-stage robust UC method [7], the reserve-based method [20] where base-case generation plan and reserves are co-optimized, and the proposed method were applied. In the reserve-based method, the base-case load scenario used is shown in Fig. 3; the maximum up and down spinning reserves of the DGs were set equal to the ramp up and down limits, respectively; the corresponding costs were 0.5 times their marginal generation costs; only a base-case operation was planned for the ESS, without considering its reserve.

As for a UC decision, the conventional two-stage robust UC method and the proposed method yielded the same solution
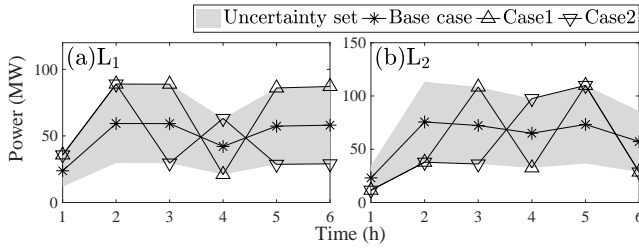
Fig. 3. Load uncertainty sets, the base-case scenario, and the tested scenarios.

where all the DGs are in operation in all the timeslots. The proposed method further yielded boxes as new operation sets of the power sources as shown in Fig. 5; the maximum power output by E_1 was zero, which indicates that E_1 does not supply power in real-time ED. In the UC solution obtained through the reserve-based method, all except G_4 are in operation, which is turned off in all the timeslots; the optimal base-case generation plans of the DGs with up and down spinning reserves are shown in Fig. 4; the optimal base-case power input and output of E_1 were zeros. No violation of power balance or transmission line constraints was expected in all the methods.

Subsequently, based on the solutions of each method, six non-anticipative single-period ED problems were solved consecutively over the planning horizon for two sets of load and DG outage scenarios, Case1 and Case2, to test their robustness under non-anticipativity. In Case1, as a setting of DG outage, DG_1 and DG_5 are assumed to fail to start. In Case2, DG_2 and DG_3 are assumed to fail to start. The load scenarios used are shown in Fig. 3. Note that the feasible ranges of variables in each single-period ED problem depend on the past ED solutions, which are now constant, whereas there is no dynamic constraint in each problem in that the variables are of the same timeslot.

For Case1, the single-period ED solution based on the UC

Fig. 4. Generation plans with reserves and single-period ED solutions for Case2. The generator G_4 was turned off intendedly and the base-case power inputs and outputs of E_1 were zeros.
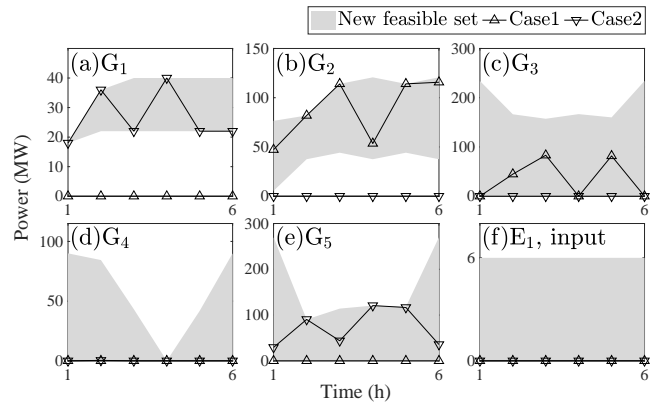
Fig. 5. Boxes as new feasible operation sets and single-period ED solutions of the power sources in them. The maximum power outputs by E_1 were zeros.

schedule obtained using the conventional two-stage robust UC method, which is shown in Fig. 6, incurred 33.9 MW of power surplus at timeslot 4. This is because the method models real-time ED as a multi-period problem. The multi-period ED solution, where the load scenario over the planning horizon as a whole is expediently assumed to be available, is shown in Fig. 6, which did not violate any constraint. The single-period and multi-period ED solutions of the power sources at timeslot 4 were the same except for G_2. In the single-period ED solution, the power output by G_2 at timeslot 4 cannot be decreased in contrast to the multi-period ED solution, causing the power imbalance. This is due to the ramp down limit. In the multi-period ED solution, the power outputs by G_2 at timeslots 3 and 5 are reduced, thus making it possible for the power output at timeslot 4 to decrease further; instead, the other more expensive power sources available, G_3 and E_1, were used at timeslots 3 and 5. The single-period ED solution obtained using the reserve-based method did not violate any constraint.

For Case2, the single-period ED solution obtained using the reserve-based method, which is shown in Fig. 4, incurred 18 MW of power shortage at timeslot 4. This is because the dynamic constraints of the DGs are considered only for the base-case generation plan and ignored for the reserves. In other

TABLE I
OPERATIONAL PARAMETERS OF DGS

Parameters	G_1	G_2	G_3	G_4	G_5
C^n ($)	0	0	0	0	0
C^{su} (k$)	14	15	30	40	10
C^{sd} ($)	12	13.5	27	36	9
C^g ($/MWh)	14	15	30	40	10
X^{max} (MW)	40	170	520	200	600
X^{min} (MW)	0	0	0	0	0
X^u, X^d, X^{su}, X^{sd} (MW/h)	18	76.5	234	90	270
T^u (h)	4	4	4	4	4
T^d (h)	3	3	3	3	3

TABLE II
OPERATIONAL PARAMETERS OF E_1

C^i ($/MWh)	C^o ($/MWh)	Y^i, Y^o (MW)	S (MWh)	S_0 (MWh)
4	4.8	6	60	0
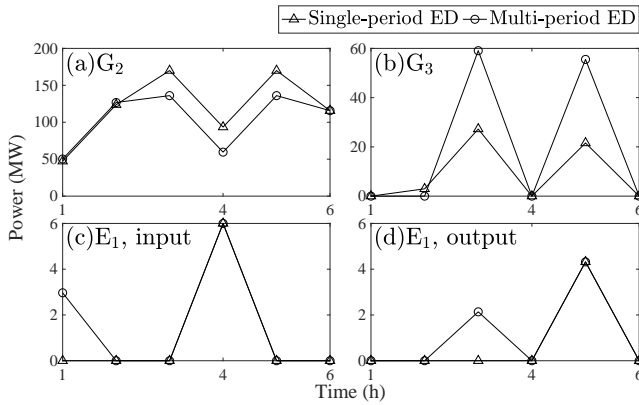
Fig. 6. Multi-period and single-period ED solutions for Case1 based on the UC solution by the conventional two-stage robust UC. The power outputs by G_4, which was turned on, were zeros.

words, the scheduled reserve at a timeslot might not be able to become fully activated owing to the ramp limits regarding the power output of DGs at the previous timeslot, as in Fig. 4(a). The single-period ED solution obtained using the conventional two-stage robust UC method did not violate any constraint.

In contrast, the proposed method did not violate any constraint for both scenarios, whose single-period ED solutions are shown in Fig. 5. This is because non-anticipative single-period ED is modeled properly in the proposed method in that the box as a new feasible set of each single-period ED problem is independent of uncertainties and ED solutions at other timeslots.

B. Computational performance

In this subsection, the computation times and numbers of iterations required by the proposed method and the conventional two-stage robust UC method are compared for a modified version of the IEEE 118-bus system [30]. The quadratic terms of the generation costs of the DGs in the original system were ignored and 5 ESSs of the same type were added to buses 1, 2, 3, 4, and 6. The maximum power output and input of each ESS were set to 8.1 MW; the power input and output efficiencies were set to 0.9 and 0.8, respectively; the storage capacity and initial stored energy were set to 80.5 MWh and 0 MWh, respectively.

As for the uncertainties, a base-case load scenario over a planning horizon of 24 timeslots was randomly generated to model the load uncertainty set, whose sum and peak value over the planning horizon were 8597.6 MW and 4065.6 MW, respectively. The maximum and minimum loads at each timeslot were set to $(1 \pm \Delta)$ times their base-case values with different values of $\Delta = 0, 0.1, 0.2, 0.3, 0.4, 0.5$. Simultaneously, different values of $\kappa = 0, 1, 2$ were applied as the contingency criterion, yielding 17 cases except the one for $(\Delta, \kappa) = (0, 0)$ where there is no uncertainty. The convergence tolerance ε in Benders decomposition was set to 1.0×10^{-3}. The time limit was set to 2 h and both methods were terminated owing to timeout when $(\Delta, \kappa) = (0.4, 2), (0.5, 2)$. The computation times and the numbers of iterations of the proposed method for the remaining 15 cases are listed in TABLE III, where

the corresponding values obtained using the conventional two-stage robust UC method are given in parentheses as well.

The proposed method required more computation time for every case except the one for $(\Delta, \kappa) = (0.1, 2)$. The reason why it requires more computation time than the conventional two-stage robust UC method is that the number of variables is always greater, i.e., it determines not only a UC schedule but also new feasible sets of the power sources. Moreover, a change in κ had a larger impact on the computation time than that of Δ for both methods. This is because different values of κ yield different cardinalities of $\mathcal{H}$, which is not the case for Δ and $\{0, 1\}^{NT}$. It can also be observed that, for the same reason, the number of iterations increased with κ but not with Δ in both methods.

C. Conservatism

In this subsection, conservatism in the proposed method is discussed for the same system and parameter settings as in the previous subsection. With the boxes as new feasible sets of real-time ED for each case of (Δ, κ), 24 single-period ED problems over the planning horizon were solved for 100 randomly generated sets of load and DG outage scenarios, except for the case of $(\Delta, \kappa) = (0, 1)$ where only 55 scenarios were used, which is the number of DGs, 54, plus one for the case where no DG fails to start. When $\Delta \geq 0.1$, the load scenarios were selected among the interior points of the load uncertainty set, which indicates that all the tested scenarios are non-worst cases. Subsequently, the deterministic UC method described in Section II-A was applied to obtain the minimum total operational costs. The results are shown in TABLE IV.

In each cell, the number in the first row represents the mean value of the actual operational costs of the proposed method for the 100 sets of scenarios in each case of (Δ, κ). The number in the second row is the mean value of the minimum operational costs; the average ratio of the actual cost to the minimum cost is given in parentheses next to it. The number in the third row is the worst-case operational cost of the proposed method; the average ratio of the actual cost to the worst-case cost is given in parentheses next to it. For reference, the

TABLE III
THE COMPUTATION TIME (s) AND NUMBER OF ITERATIONS

Parameters	$\kappa = 0$	$\kappa = 1$	$\kappa = 2$
$\Delta = 0.0$	-	66.183 (43.093) 3 (3)	470.531 (48.082) 8 (8)
$\Delta = 0.1$	41.208 (20.609) 2 (2)	140.772 (47.194) 5 (5)	244.699 (403.773) 6 (6)
$\Delta = 0.2$	40.563 (20.757) 2 (2)	180.120 (47.041) 4 (4)	1250.745 (239.882) 6 (6)
$\Delta = 0.3$	41.543 (21.128) 2 (2)	326.325 (50.233) 7 (7)	2345.753 (1109.202) 7 (7)
$\Delta = 0.4$	42.376 (21.348) 2 (2)	203.185 (50.541) 5 (5)	Timeout
$\Delta = 0.5$	46.867 (21.823) 2 (2)	420.348 (87.478) 4 (4)	Timeout

results for the case of $(\Delta, \kappa) = (0, 0)$ were obtained using the deterministic UC method and are shown in the table as well.

The average ratio of the actual cost of the proposed method to the minimum value increased with both Δ and κ. This indicates that, the larger Δ or κ was, the more conservative the solution of the proposed method was, which makes the real-time ED solution less optimal, i.e., more expensive. Moreover, the worst-case cost increased with both Δ and κ, as can be expected.

As for the suboptimality of the non-worst-case ED solutions, notably, a larger uncertainty set does not always lead to a larger feasible operation set of a power source in the proposed method. More generally, the shape of a box as a new feasible operation set is rather arbitrary. For example, in the above experiment, the feasible generation ranges of the DG at bus 5 at timeslot 7 for the cases of $(\Delta, \kappa) = (0.1, 0)$ and of $(\Delta, \kappa) = (0.2, 0)$ were $[550, 550]$ MW, which is a degenerate interval, and $[110, 517.6]$ MW, respectively; the two intervals do not show any inclusion relationship. This is because the proposed method minimizes the worst-case total operational cost and does not consider the optimality of a non-worst-case ED solution. In this sense, the suboptimality of a non-worst-case ED solution can be reduced by expanding the box inside the original feasible operation set. The box-expanding method is beyond the scope of this paper and will be reported separately.

V. CONCLUSION

An approach for non-anticipative two-stage robust UC was proposed, where a feasible region of a real-time ED problem at each timeslot is predetermined with a UC schedule. The bottom line is that a multi-period ED problem, which is nested in a conventional two-stage robust UC problem, is decomposed into single-period ED problems, each of which corresponds to

TABLE IV
THE AVERAGE ACTUAL COST (M\$), AVERAGE MINIMUM COST (M\$), AND WORST-CASE COST (M\$)

Parameters	$\kappa = 0$	$\kappa = 1$	$\kappa = 2$
$\Delta = 0.0$	1.7355 1.7355 (1.0000) 1.7355 (1.0000)	1.7395 1.7356 (1.0023) 1.7395 (1.0000)	1.7455 1.7356 (1.0057) 1.7455 (1.0000)
$\Delta = 0.1$	1.7424 1.7406 (1.0010) 1.9095 (0.9125)	1.7431 1.7355 (1.0044) 1.9155 (0.9100)	1.7534 1.7377 (1.0090) 1.9235 (0.9116)
$\Delta = 0.2$	1.7240 1.7209 (1.0018) 2.0834 (0.8275)	1.7466 1.7360 (1.0061) 2.0914 (0.8351)	1.7554 1.7351 (1.0117) 2.1014 (0.8353)
$\Delta = 0.3$	1.7471 1.7419 (1.0030) 2.2594 (0.7733)	1.7627 1.7475 (1.0087) 2.2694 (0.7767)	1.7863 1.7400 (1.0266) 2.3270 (0.7676)
$\Delta = 0.4$	1.7431 1.7351 (1.0046) 2.4353 (0.7158)	1.7593 1.7364 (1.0132) 2.4515 (0.7176)	-
$\Delta = 0.5$	1.7389 1.7265 (1.0072) 2.6133 (0.6654)	1.7541 1.7015 (1.0310) 2.6957 (0.6507)	

a real-time ED problem. Future research directions include the development of convergence acceleration techniques for the proposed method.

APPENDIX

If $\mathcal{D}$ is a general convex polytope, its vertices cannot be easily identified and the subproblem in Benders decomposition is not equivalently reformulated as an MILP problem. In this case, the outer approximation (OA) method [7], [28] can be applied to convert the bilinear term regarding d and ξ^3 to a real variable θ with iteratively added constraints, each of which represents its linearization around a transient solution. The OA method for solving the subproblem is described as follows.

For initialization, select any vertex d_0 in $\mathcal{D}$ as an initial guess for d. Subsequently, solve the problem

$$\max_{h \in \mathcal{H}, \xi \in \Xi, \zeta^1 \in Z(h, \xi^1)} C_6^{\mathrm{T}} \left(\hat{x}_K, \hat{y}_K, \zeta^1, \xi^2, \xi^3 \right) - (E d_0)^{\mathrm{T}} \xi^3$$

where

$$C_6 \left(\hat{x}_K, \hat{y}_K, \zeta^1, \xi^2, \xi^3 \right) := \\ - a^{\mathrm{T}} \left(\hat{x}_K, \mathbf{1} \right) \zeta^1 - b^{\mathrm{T}} \left(\hat{y}_K \right) \xi^2 - e^{\mathrm{T}} \xi^3$$

to obtain the solution ξ_0^3 corresponding to ξ^3. For each iteration step $J \geq 1$, solve

$$\max_{d \in \mathcal{D}, h \in \mathcal{H}, \xi \in \Xi, \zeta^1 \in Z(h, \xi^1), \theta} C_6^{\mathrm{T}} \left(\hat{x}_K, \hat{y}_K, \zeta^1, \xi^2, \xi^3 \right) + \theta \\ \text{s.t.} \quad \theta \leq L \left(d_j, \xi_j^3 \right), \quad j = 0, 1, \ldots, J - 1 \quad (17)$$

where $L \left(d_j, \xi_j^3 \right) := \left(E d_j \right)^{\mathrm{T}} \xi_j^3 - \left(E d \right)^{\mathrm{T}} \xi_j^3 - \left(E d_j \right)^{\mathrm{T}} \xi^3$ is the linearization of the bilinear term $-\left(E d \right)^{\mathrm{T}} \xi^3$ around $d = d_j$ and $\xi^3 = \xi_j^3$. Let d_J and UB_J^2 denote the solution corresponding to d and the optimal value of the problem (17), respectively. Subsequently, solve

$$\max_{\substack{h \in \mathcal{H}, \xi \in \Xi, \\ \zeta^1 \in Z(h, \xi^1)}} C_6^{\mathrm{T}} \left(\hat{x}_K, \hat{y}_K, \zeta^1, \xi^2, \xi^3 \right) - (E d_J)^{\mathrm{T}} \xi^3 \quad (18)$$

to obtain the solutions h_J and ξ_J corresponding to h and ξ, respectively. Let LB_J^2 denote the optimal value. If $UB_J^2 - LB_J^2 < \varepsilon^2$, where ε^2 is a convergence tolerance, the iteration stops and d_K, h_K, and ξ_K are set to d_J, h_J, and ξ_J, respectively; otherwise, J increases to $J + 1$ and the problems (17) and (18) are solved again.

REFERENCES

[1] Q. Wang, J. Wang, and Y. Guan, "Stochastic unit commitment with uncertain demand response," *IEEE Transactions on power systems*, vol. 28, no. 1, pp. 562–563, 2013.

[2] A. Papavasiliou and S. S. Oren, "Multiarea stochastic unit commitment for high wind penetration in a transmission constrained network," *Operations Research*, vol. 61, no. 3, pp. 578–592, 2013.

[3] J. F. Benders, "Partitioning procedures for solving mixed-variables programming problems," *Numerische mathematik*, vol. 4, no. 1, pp. 238–252, 1962.

[4] Q. P. Zheng, J. Wang, P. M. Pardalos, and Y. Guan, "A decomposition approach to the two-stage stochastic unit commitment problem," *Annals of Operations Research*, vol. 210, no. 1, pp. 387–410, 2013.

[5] L. Wu and M. Shahidehpour, "Accelerating the benders decomposition for network-constrained unit commitment problems," *Energy Systems*, vol. 1, no. 3, pp. 339–376, 2010.

[6] R. Jiang, J. Wang, and Y. Guan, "Robust unit commitment with wind power and pumped storage hydro," *IEEE Transactions on Power Systems*, vol. 27, no. 2, pp. 800–810, 2012.

[7] D. Bertsimas, E. Litvinov, X. A. Sun, J. Zhao, and T. Zheng, "Adaptive robust optimization for the security constrained unit commitment problem," *IEEE Transactions on Power Systems*, vol. 28, no. 1, pp. 52–63, 2013.

[8] G. Liu and K. Tomsovic, "Robust unit commitment considering uncertain demand response," *Electric Power Systems Research*, vol. 119, pp. 126–137, 2015.

[9] C. Zhao, J. Wang, J.-P. Watson, and Y. Guan, "Multi-stage robust unit commitment considering wind and demand response uncertainties," *IEEE Transactions on Power Systems*, vol. 28, no. 3, pp. 2708–2717, 2013.

[10] M. Melamed, A. Ben-Tal, and B. Golany, "A multi-period unit commitment problem under a new hybrid uncertainty set for a renewable energy source," *Renewable Energy*, vol. 118, pp. 909–917, 2018.

[11] C. Zhao and Y. Guan, "Unified stochastic and robust unit commitment," *IEEE Transactions on Power Systems*, vol. 28, no. 3, pp. 3353–3361, 2013.

[12] G. Morales-Espana, Á. Lorca, and M. M. de Weerdt, "Robust unit commitment with dispatchable wind power," *Electric Power Systems Research*, vol. 155, pp. 58–66, 2018.

[13] A. Street, F. Oliveira, and J. M. Arroyo, "Contingency-constrained unit commitment with $n - k$ security criterion: A robust optimization approach," *IEEE Transactions on Power Systems*, vol. 26, no. 3, pp. 1581–1590, 2011.

[14] Q. Wang, J.-P. Watson, and Y. Guan, "Two-stage robust optimization for n-k contingency-constrained unit commitment," *IEEE Transactions on Power Systems*, vol. 28, no. 3, pp. 2366–2375, 2013.

[15] P. Xiong and P. Jirutitijaroen, "An adjustable robust optimization approach for unit commitment under outage contingencies," in *Power and Energy Society General Meeting, 2012 IEEE*. IEEE, 2012, pp. 1–8.

[16] Q. P. Zheng, J. Wang, and A. L. Liu, "Stochastic optimization for unit commitment—a review," *IEEE Transactions on Power Systems*, vol. 30, no. 4, pp. 1913–1924, 2015.

[17] B. Hu, L. Wu, X. Guan, F. Gao, and Q. Zhai, "Comparison of variant robust scuc models for operational security and economics of power systems under uncertainty," *Electric Power Systems Research*, vol. 133, pp. 121–131, 2016.

[18] J. Wang, M. Shahidehpour, and Z. Li, "Security-constrained unit commitment with volatile wind power generation," *IEEE Transactions on Power Systems*, vol. 23, no. 3, pp. 1319–1327, 2008.

[19] W. Wei, F. Liu, S. Mei, and Y. Hou, "Robust energy and reserve dispatch under variable renewable generation," *IEEE Transactions on Smart Grid*, vol. 6, no. 1, pp. 369–380, 2015.

[20] N. G. Cobos, J. M. Arroyo, and A. Street, "Least-cost reserve offer deliverability in day-ahead generation scheduling under wind uncertainty and generation and network outages," *IEEE Transactions on Smart Grid*, 2016.

[21] L. Wu, M. Shahidehpour, and T. Li, "Stochastic security-constrained unit commitment," *IEEE Transactions on Power Systems*, vol. 22, no. 2, pp. 800–811, 2007.

[22] S. Takriti, B. Krasenbrink, and L. S.-Y. Wu, "Incorporating fuel constraints and electricity spot prices into the stochastic unit commitment problem," *Operations Research*, vol. 48, no. 2, pp. 268–280, 2000.

[23] Y. Wang, Q. Xia, and C. Kang, "Unit commitment with volatile node injections by using interval optimization," *IEEE Transactions on Power Systems*, vol. 26, no. 3, pp. 1705–1713, 2011.

[24] A. Lorca, X. A. Sun, E. Litvinov, and T. Zheng, "Multistage adaptive robust optimization for the unit commitment problem," *Operations Research*, vol. 64, no. 1, pp. 32–51, 2016.

[25] A. Lorca and X. A. Sun, "Multistage robust unit commitment with dynamic uncertainty sets and energy storage," *IEEE Transactions on Power Systems*, vol. 32, no. 3, pp. 1678–1688, 2017.

[26] H. Ibrahim, A. Ilinca, and J. Perron, "Energy storage systems characteristics and comparisons," *Renewable and sustainable energy reviews*, vol. 12, no. 5, pp. 1221–1250, 2008.

[27] A. Bemporad and M. Morari, "Control of systems integrating logic, dynamics, and constraints," *Automatica*, vol. 35, no. 3, pp. 407–427, 1999.

[28] M. A. Duran and I. E. Grossmann, "An outer-approximation algorithm for a class of mixed-integer nonlinear programs," *Mathematical programming*, vol. 36, no. 3, pp. 307–339, 1986.

[29] B. Zeng and L. Zhao, "Solving two-stage robust optimization problems using a column-and-constraint generation method," *Operations Research Letters*, vol. 41, no. 5, pp. 457–461, 2013.

[30] R. D. Zimmerman, C. E. Murillo-Sánchez, and R. J. Thomas, "Matpower: Steady-state operations, planning, and analysis tools for power systems research and education," *IEEE Transactions on power systems*, vol. 26, no. 1, pp. 12–19, 2011.

Youngchae Cho received his B.S. and M.S. degrees in Engineering from Tokyo Institute of Technology, Tokyo, Japan, in 2017 and 2018, respectively. He is currently pursuing a Ph.D. degree in Engineering at Tokyo Institute of Technology. His research interests include optimization under uncertainty and its application to power system operation.

Takayuki Ishizaki (S'10-M'12) was born in Aichi, Japan, in 1985. He received the B.Sc., M.Sc., and Ph.D. degrees in Engineering from Tokyo Institute of Technology, Tokyo, Japan, in 2008, 2009, and 2012, respectively. He served as a Research Fellow of the Japan Society for the Promotion of Science from April 2011 to October 2012. From October to November 2011, he was a Visiting Student at Laboratoire Jean Kuntzmann, Universite Joseph Fourier, Grenoble, France. From June to October 2012, he was a Visiting Researcher at School of Electrical Engineering, Royal Institute of Technology, Stockholm, Sweden. Since November 2012, he has been with the Department of Mechanical and Environmental Informatics, Graduate School of Information Science and Engineering, Tokyo Institute of Technology, where he is currently an Assistant Professor. His research interests include network model reduction and its applications, retrofit control and its applications, and optimal scheduling and market design for smart grids. Dr. Ishizaki is a member of IEEE, SICE, and ISCIE. He was a finalist of the 51st IEEE CDC Best Student-Paper Award.

Nacim Ramdani (M'08) received the Engineer degree from Ecole Centrale de Paris, France, in 1990, the Ph.D. degree from the Université Paris-Est Créteil, France, in 1994 and the Habilitation in 2005. Since September 2010, he has been a Full Professor at the Université d'Orléans (IUT de Bourges) affiliated with the Laboratoire PRISME EA 4229 Université of Orléans - INSA Centre Val de Loire. From 1996 to 2010, he was Maître de Conférences with the Université Paris-Est Créteil. He was affiliated with the LIRMM CNRS Montpellier during 2005-2010 and also on secondment with the INRIA during 2007-2009. He is the co-Chair of the workgroup group on Verification and Synthesis of Cyber-Physical Systems within the French research group on Automatic Control (GDR MACS). His current research interests revolve around modelling, analysis, and estimation of non-linear and hybrid systems, and their applications. He mainly focuses on interval methods and set computation techniques.
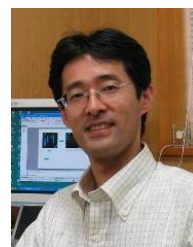
Jun-ichi Imura (M'93-SM'18) received the M.E. degree in applied systems science and the Ph.D. degree in mechanical engineering from Kyoto University, Kyoto, Japan, in 1990 and 1995, respectively. Since 2001, he has been with Tokyo Institute of Technology, Tokyo, Japan, where he is currently a Professor of School of Engineering. He served as an Associate Editor of Automatica (2009-2017), the Nonlinear Analysis: Hybrid Systems (2011-2016), and IEEE Trans. on Automatic Control (2014-2016). He is a member of SICE, ISCIE, and The Robotics Society of Japan.